



**HAL**  
open science

## Sclareol purification using the supercritical fractionation process: A modeling case study

C. Dufour, Christelle Crampon, C. Delbecque, P-P. Garry, Elisabeth Badens

### ► To cite this version:

C. Dufour, Christelle Crampon, C. Delbecque, P-P. Garry, Elisabeth Badens. Sclareol purification using the supercritical fractionation process: A modeling case study. *Journal of Supercritical Fluids*, 2020, 159, pp.104754. 10.1016/j.supflu.2020.104754 . hal-02892487

**HAL Id: hal-02892487**

**<https://hal.science/hal-02892487v1>**

Submitted on 7 Mar 2022

**HAL** is a multi-disciplinary open access archive for the deposit and dissemination of scientific research documents, whether they are published or not. The documents may come from teaching and research institutions in France or abroad, or from public or private research centers.

L'archive ouverte pluridisciplinaire **HAL**, est destinée au dépôt et à la diffusion de documents scientifiques de niveau recherche, publiés ou non, émanant des établissements d'enseignement et de recherche français ou étrangers, des laboratoires publics ou privés.



Distributed under a Creative Commons Attribution - NonCommercial 4.0 International License



26 which is a raw material used in perfumery for the production of Ambrox® or Ambroxan®  
27 [3,4]. Sclareol (fig. 1) is used as a base and fixative note with a view to substituting natural  
28 ambergris (whale intestinal secretions).

29 The aim of this study was to carry out the modeling of experimental data obtained by  
30 fractionating a clary sage complex mixture containing 24% of sclareol and about 200 other  
31 compounds, using supercritical CO<sub>2</sub>, with a simple method already applied to supercritical  
32 fractionation results [5].

33 Very little modeling of the supercritical fractionation process according to this approach is  
34 proposed in the literature. Mathematical models do not often take into account the physical  
35 phenomena such as the model used by Varona *et al.* [6]. Other models, such as Martín and  
36 Cocero's, study the purification of one single compound [7]. To carry out this modeling, the  
37 choice fell upon a simple model called the group method, which was developed by Kremser  
38 [8] for absorbers and improved by Edminster [9] for vapor/liquid separations under low  
39 pressure. Henley and Seader [10] then applied this method to the vapor/liquid separation of  
40 hydrocarbons. More recently, Pieck *et al.* [5] used the group method to represent the  
41 supercritical fractionation of an esterified fish oil.

42 The supercritical fractionation is a process allowing the compounds contained in a liquid  
43 mixture to be separated by using a solvent under supercritical conditions. The feed diluent and  
44 the solvent must not be miscible under the implemented operating conditions. Supercritical  
45 fractionation process is generally carried out in continuous mode, using a counter-current  
46 packed column, in which the liquid feed and the supercritical solvent are introduced at the top  
47 and bottom of the column respectively, and put in contact with each other [11,12]. In this  
48 configuration, supercritical fractionation is similar to absorption where the extract (or light  
49 phase) composed of the most soluble compounds in the supercritical solvent is recovered at  
50 the top of the column. Conversely, the raffinate, corresponding to the highest density phase

51 containing the least soluble compounds, is collected at the bottom of the column. Carbon  
52 dioxide (CO<sub>2</sub>) is the most frequently encountered solvent for the supercritical fractionation  
53 operation and allows such a process to cumulate many advantages when compared to  
54 conventional techniques. First of all, supercritical CO<sub>2</sub> fractionation is a sustainable and  
55 continuous process. The process selectivity can be tuned according to the pressure and  
56 temperature conditions applied in the column, which are directly linked to the physico-  
57 chemical properties of supercritical CO<sub>2</sub>, and according to the feed and solvent flowrates on  
58 which the hydrodynamics depends. CO<sub>2</sub> can be easily recycled and the raffinate and the  
59 extracts are free of solvent since gaseous CO<sub>2</sub> is spontaneously separated after  
60 depressurization. A post-treatment is generally not required. Even if supercritical fractionation  
61 involves high pressure equipment, it can be economically viable thanks to its compacity and  
62 flexibility. In addition, it is a low temperature operation which allows processing thermolabile  
63 compounds. To conclude, supercritical CO<sub>2</sub> fractionation can be an interesting alternative for  
64 complex separations [13]. Finally, this operation can also be coupled with conventional ones  
65 to improve their overall separation efficiency.

66 In this work, an experimental study followed by a modeling stage is proposed. In the first  
67 step, experiments were conducted at pressures of (10 to 12) MPa, at temperatures of (313 to  
68 338) K and for solvent-over-feed ratios between 13 and 173 with the objective of obtaining a  
69 sclareol-rich raffinate, the solubility of sclareol in supercritical CO<sub>2</sub> being low. These  
70 operating conditions were determined after a preliminary study presented in a previous article  
71 [14]. In the second step, the group method was used to model the distribution of sclareol and  
72 11 selected compounds in extract and raffinate during the supercritical CO<sub>2</sub> fractionation  
73 process. The assumptions for the model application were checked and the number of  
74 theoretical stages and the distribution factors for each selected compound were adjusted on

75 experimental composition data. Finally, the calculated compositions in raffinate and extracts  
76 were compared to the experimental ones.

77

## 78 **2. Materials and Methods**

### 79 **2.1. Materials**

80 Carbon dioxide with a purity of 99.7% was supplied by Linde Gaz (France).

81 The studied feed used for supercritical CO<sub>2</sub> fractionation experiments was provided by the  
82 company Bontoux SAS (Saint Auban sur l'Ouvèze, France). This liquid mixture was the  
83 lightest fraction of an extract obtained from Clary sage flowers and was composed of 24 wt%  
84 of sclareol as well as about 200 other compounds.

85

### 86 **2.2. Experimental set-up**

87 Fig. 2 shows a simplified schematic diagram of the supercritical CO<sub>2</sub> fractionation apparatus.  
88 The apparatus and procedure have already been described in a previous paper [14]. The unit  
89 consists in a 2.6 m high packed column with a 30 mm internal diameter.

90 A typical run was carried out as follows: the column was first heated up to the targetted  
91 temperature before CO<sub>2</sub> was introduced. A CO<sub>2</sub> high-pressure piston pump was then set at the  
92 desired flow rate and operating pressure by means of a back-pressure regulator. When the  
93 steady-state was installed relative to CO<sub>2</sub>, the liquid mixture was introduced at the desired  
94 flow rate using a piston pump. Extract and raffinate samples were collected and analyzed at  
95 regular time intervals and steady-state conditions were assumed to be reached as soon as the  
96 standard deviations for three successive samples were less than 1wt% of sclareol. After  
97 repeatability tests, the experimental raffinate and extract compositions were determined with  
98 an uncertainty around 2.6% and the error on the ratio S/Z (solvent massic flowrate divided by  
99 the liquid mixture massic flowrate) was about 3%.

100 Experimental data were obtained for operating conditions as follows: temperatures between  
101 313 K and 338 K, pressures between 10 MPa and 12 MPa and for solvent-over-feed ratios  
102 between 13 and 173. These operating conditions were deduced after a preliminary study  
103 presented in a previous article [14]. The objective was to find the optimum operating  
104 conditions for concentrating sclareol in the raffinate.

105

### 106 **2.3. Analytical methods**

107 The process input (feed mixture) and outputs (extract and raffinate collected through the  
108 fractionation experiments) were analyzed by gas chromatography with a column HB5HT: 15  
109 m × 0.25 mm × 0.1 μm with Flame Ionization Detector (FID) (Autosystem XL, Perkin  
110 Elmer). The recovered extract and the liquid feed mixture were diluted to 20% in chloroform  
111 (Sodipro, 99.5%). Diethyl phthalate (Grasse Chimie's World, 99.5%) was used as a standard  
112 for the quantification of sclareol.

113

### 114 **2.4. Modeling**

115 The extract and raffinate compositions were calculated using a model based on the group  
116 method developed by Kremser and Edmister [8] for the modeling absorption process. The  
117 choice fell on this model because it had already been validated on the experimental results of  
118 Pieck *et al.* [5].

119 The model is based on a simple relation linking the extraction yield ( $\varepsilon$ ) and the stripping  
120 factor ( $\xi_i$ ) for each component  $i$  (Eq. 1).

$$121 \quad \xi_i = K_i \varepsilon \quad (1)$$

122 Where  $K_i$  is the overall distribution coefficient of component  $i$ , and  $\varepsilon$ , the extraction yield, is  
123 the ratio between the extract mass flow rate  $E$  and the feed mass flow rate  $Z$ . The extraction

124 yield  $\varepsilon$  is calculated as follows (Eq. 2), considering that the feed mass flowrate  $Z$  is equal to  
 125 the sum of the extract mass flow rate  $E$  and the raffinate mass flow rate  $R$ :

$$126 \quad \varepsilon = \frac{E}{Z} = \frac{E}{E+R} \quad (2)$$

127 The stripping loss was determined by (Eq. 3):

$$128 \quad \varphi_{s,i} = \frac{(1-\varepsilon)(\xi_i-1)}{\xi_i^n(\xi_i-\varepsilon)+(1-\varepsilon)} \quad (3)$$

129 The expression shown as eq. 3 can be used to compute the extract and raffinate compositions  
 130 (respectively  $X^E$  and  $X^R$ ) if the stripping loss for each component  $i$  is known.

$$131 \quad X_i^E = \frac{(1-\varphi_{s,i})X_i^Z}{1-\varphi_{s,j}X_j^Z} \quad (4)$$

$$132 \quad X_i^R = \frac{\varphi_{s,i}X_i^Z}{\varphi_{s,j}X_j^Z} \quad (5)$$

133  $X^Z$  is the composition of compound  $i$  in the feed.

134 The error distribution in the experimental data was assumed to be log-normal. Hence, the  
 135 number of theoretical stages  $n$  and the overall distribution ratio  $K_i$  were fitted altogether to  
 136 experimental data using the GRG (Generalized Reduced Gradient) nonlinear Solving Method  
 137 from the Microsoft Excel solver, by minimizing the objective function (Eq. 6):

$$138 \quad f = \sum_{vi} \left( \ln(X_i^{exp}) - \ln(X_i^{calc}) \right)^2 \quad (6)$$

139 In which  $X_i$  represents both the extract and raffinate mass fractions of the selected components  
 140  $i$  and the rest of the compounds cumulated into a single pseudo-component.

141 Modeling using the group method requires the validation of two hypotheses: that the steady-  
 142 state is established and the studied mixture is considered as ideal.

143

## 144 **3. Results and discussion**

### 145 **3.1. Experimental results**

146 For each experimental condition, the overall mass balance in sclareol was satisfactory since  
147 the mean deviation was 2%. For all experiments, the compound of interest, sclareol, was  
148 concentrated in the raffinate. Table 1 gives the experimental results obtained for the operating  
149 conditions studied.

150  $Z$ ,  $S$ ,  $R$ , and  $E$ , are the mass flow rates of the feed, supercritical CO<sub>2</sub>, raffinate, and extract,  
151 respectively.  $X^Z$  is the mass fraction of sclareol in the feed and  $X^R$ , and  $X^E$ , are the supercritical  
152 solvent-free mass fractions of sclareol in the raffinate and the extract, respectively.  $\beta^*$  is the  
153 ratio between the recalculated mass fraction of sclareol in the feed from a partial mass balance  
154 when the steady state was assumed, and the initial mass fraction in the feed. Finally,  $\tau$  is the  
155 sclareol yield in the raffinate.

156 Figs. 3 to 5 regroup the results obtained and highlight the influence of pressure, temperature,  
157 and CO<sub>2</sub>-over-feed ratio ( $S/Z$ ) on the mass fraction of sclareol (a) in the extract and in the  
158 raffinate, and on the sclareol yield (b) in the raffinate.

159 Fig. 3 (a) illustrates the influence of temperature on the mass fraction of sclareol at a pressure  
160 set to 10 MPa, as a function of the CO<sub>2</sub>-over-feed mass ratio. Assays were conducted at three  
161 temperatures 313 K, 323 K and 333 K. At a constant CO<sub>2</sub>-over-feed ratio, a decrease in  
162 temperature led to an increase in the mass fraction of sclareol in the raffinate. However, a  
163 slight increase in the content of sclareol in the extract was also noted. This behavior appears  
164 clearly in Fig. 3 (b) which shows the evolution of the sclareol yield in the raffinate versus the  
165 ratio  $R/(E+R)$ . At 10 MPa, a decrease in the temperature thus led to a decrease in the  
166 selectivity. Experiments at 313 K were thus no longer conducted in order to avoid the sharing  
167 of sclareol between the raffinate and the extract. Moreover, at 313 K, it was not possible to  
168 work at a CO<sub>2</sub>-over-feed mass ratio bigger than 40. Above this value, no raffinate was  
169 withdrawn, maybe due to a partial crystallization of the sclareol in the column.



170 Fig. 4 and 5 show the influence of pressure at two temperatures: 323 K and 338 K. Fig. 4 (a)  
171 highlights that a 338 K pressure had a slight influence on the mass fraction of sclareol in the  
172 extract, whatever the CO<sub>2</sub>-over-feed ratio from 15 up to 160. The influence of pressure was a  
173 little more pronounced on the sclareol content in the raffinate since at a constant CO<sub>2</sub>-over-  
174 feed ratio, the mass fraction of sclareol at 12 MPa is slightly higher than at both 10 MPa and  
175 11 MPa. Even in Fig. 4 (b) which illustrates the evolution of the sclareol yield versus the ratio  
176  $R/(R+E)$ , no significant influence of pressure was noted.

177 Some assays were finally carried out at 323 K (Fig. 5). At that temperature, the pressure had a  
178 significant influence on the mass fraction of sclareol both in the raffinate and the extract. At  
179 the highest pressure of 12 MPa, Fig. 5 (b) reveals the fall in sclareol yield while the ratio  
180  $R/(R+E)$  decreased. As for the temperature of 313 K, at 323 K there was a drop in the  
181 selectivity when the pressure increased.

182

### 183 **3.2 Selection of the 12 compounds from the feed selected for modeling**

184 The liquid mixture to be fractionated was composed of about 200 different compounds. In this  
185 work, 12 compounds including sclareol were selected to study their distribution in the extract  
186 and in the raffinate versus the extraction yield. The choice fell on compounds easily  
187 identifiable by gas chromatography, distributed over the entire length of the chromatogram,  
188 having interesting behavior for sclareol purification, and present both in the extract and the  
189 raffinate. Sclareol (I<sub>12</sub>), together with seven major compounds (named I<sub>1</sub> to I<sub>7</sub>) were identified  
190 as major compounds in the mixture. Four impurities (named I<sub>8</sub> to I<sub>11</sub>) characterized the quality  
191 of the separation since they are due to the degradation of sclareol during storage and prove  
192 difficult to remove by currently used purification techniques. Fig. 6 shows the gas  
193 chromatographic profile of the feed in which the selected compounds are highlighted and  
194 table 2 gives the content of the selected compounds in the feed.

195

### 196 3.3. Assumptions for model application

197 The first assumption to be checked is that the steady-state was well established. To that aim,  
198 the mass balance for each component  $i$  in the feed should be verified:

$$199 \quad Z_i = E_i + R_i \quad (5)$$

200 With  $Z_i$ ,  $E_i$  and  $R_i$  the massic flow rates of compound  $i$  in the feed, extract and raffinate,  
201 respectively.

202 The following equation is obtained:

$$203 \quad X_i^Z = X_i^E \varepsilon + X_i^R (1 - \varepsilon) \quad (7)$$

204 The right term represents the global composition of the  $X_i^Z$  feed calculated using the mass  
205 fraction measured in the extract  $X_i^E$  and in the raffinate  $X_i^R$ . This calculated value has to be  
206 compared to the experimental one. If the mass balance is verified, when plotting the  
207 calculated mass fraction in the feed versus the experimental corresponding value, a straight  
208 line passing through the origin and with a slope of 1 is obtained. Fig. 7 shows the calculated  
209  $(X_i^Z)_{calc}$  versus the experimental  $(X_i^Z)_{exp}$  and thus illustrates the mass balance obtained for the  
210 selected components at 10 MPa and 323 K. As a proportionality is observed between the  
211 calculated and the experimental mass fractions, with in addition a slope of the straight line  
212 very close to 1, the steady-state was well established.

213 The second assumption to be checked for the application of the model is that the studied  
214 mixture can be considered as an ideal mixture, meaning that the solubility of each compound  
215 in CO<sub>2</sub> is independent of the proportion of each compound in the mixture. If the solubility is  
216 considered independent of the composition, the extraction yield is a linear function of the  
217 solvent-over-feed ratio ( $S/Z$ ). This hypothesis was checked for three studied operating  
218 conditions: a temperature of 323 K for pressures of 10 MPa and 11 MPa and a temperature of

219 338 K for a pressure of 12 MPa. Fig. 8 shows the extraction yield versus the CO<sub>2</sub>-over-feed  
220 ratio for experiments carried out at 323 K and 10 MPa. A straight line of equation ( $y = 0.004$   
221  $x$ ) was obtained leading to the conclusion that the feed mixture could be considered as ideal  
222 under such operating conditions.

223

#### 224 **3.4. Modeling of the extract and raffinate compositions**

225 The model was applied for three different operating conditions that respected the assumptions  
226 of the model (323 K for pressures of 10 MPa and 11 MPa and 338 K for a pressure of 12  
227 MPa) and table 3 gives the estimation of overall distribution coefficient ( $K$ ) for each  
228 compound and each operating condition. Fig. 9 shows the modeling of the 12 compounds  
229 selected in the mixture.

230 The estimation of the distribution coefficients in table 3 and the curves obtained in Fig. 9  
231 emphasize three different types of behavior. Firstly, compounds I1, I2, I3, I4 and I6 behaved  
232 similarly (Fig. 9 (a-d) and (e)). Indeed, they had a distribution coefficient greater than 1 so  
233 that they were preferentially collected in the extract. On the contrary, compounds I7, I8, I9,  
234 I10, I11, and the sclareol had a distribution coefficient lower than 1; they were indeed  
235 collected in the raffinate (Fig. 9 (f-l)). And finally, a third type of behavior was observed:  
236 compound I5 had a distribution coefficient around 1 and was evenly distributed between the  
237 extract and the raffinate (Fig. 9 (e)).

238 Experimental data were represented by the model with a relative error of about 15% which is  
239 satisfactory regarding the complexity of the system. Indeed, it was a natural extract with a real  
240 industrial application. The same error of 15% was determined by Pieck *et al.* [5]. Varona *et*  
241 *al.* [6] predicted the separation factor with an average deviation of 20%. Fig. 10 compares the  
242 experimental composition values to the calculated ones for the three operating conditions  
243 considered and for the 12 selected compounds. A good correlation was observed between the

244 model and the experimental data. The points outside the outline were those corresponding to  
245 traces of the light compounds in the raffinate, implying a bigger error between the model and  
246 the experimental data.

#### 247 **4. Conclusion**

248 Supercritical CO<sub>2</sub> fractionation was applied to a complex feed mixture containing more than  
249 200 compounds with the objective of concentrating sclareol in the raffinate. The group  
250 method was used in order to model the compositions of 12 selected compounds including  
251 sclareol. Although such a model may only suit ideal mixtures, a good correlation was  
252 obtained between experimental compositions and calculated values for three different  
253 operating conditions. A relative error of about 15% was reached and for such a complex  
254 system, those results can be considered as satisfactory. Moreover, modeling allowed to  
255 highlight three different types of behavior in relation to the values of the distribution  
256 coefficients. Compounds having a distribution coefficient greater than 1 were preferentially  
257 collected in the extract; when the distribution coefficients were lower than 1, the compounds  
258 were collected in the raffinate; and, finally, the compounds fairly distributed between the  
259 extract and the raffinate had distribution coefficients close to 1. Such modeling, although its  
260 simplicity, may offer a better understanding of component behavior when considering the  
261 separation of complex mixtures using supercritical fractionation.

262

#### 263 **References**

264 [1] D.C. Hao, S.L. Chen, A. Osbourn, V.G. Kontogianni, L.W. Liu, M.J. Jordán, Temporal  
265 transcriptome changes induced by methyl jasmonate in *Salvia sclarea*, *Gene* 558 (2015)  
266 41-53. <http://dx.doi.org/10.1016/j.gene.2014.12.043>.

267 [2] J.C. Caissard, T. Olivier, C. Delbecq, S. Palle, P-P. Garry, A. Audran, N. Valot, S.  
268 Moja, F. Nicolè, J-L. Magnard, S. Legrand, S. Baudino, F. Jullien, Extracellular Localization  
269 of the Diterpene Sclareol in Clary Sage (*Salvia sclarea* L., Lamiaceae), PLoS ONE 7 (2012)  
270 e48253. <https://doi.org/10.1371/journal.pone.0048253>.

271 [3] A. Caniard, P. Zerbe, S. Legrand, A. Cohade, N. Valot, J-L. Magnard, J. Bohlmann, L.  
272 Legendre, Discovery and functional characterization of two diterpene synthases for sclareol  
273 biosynthesis in *Salvia sclarea* (L.) and their relevance for perfume manufacture, BMC Plant  
274 Biol. 12 (2012) 119-132. <https://doi.org/10.1186/1471-2229-12-119>.

275 [4] C. Schmiderer, P. Grassi, J. Novak, M. Weber, C. Franz, Diversity of essential oil glands  
276 of clary sage (*Salvia sclarea* L., Lamiaceae), Plant Biol. 10 (2008) 433-440.  
277 <https://doi.org/10.1111/j.1438-8677.2008.00053.x>

278 [5] C.A. Pieck, C. Crampon, F. Charton, E. Badens, A new model for the fractionation of fish  
279 oil FAEE, J. Supercrit. Fluids 120 (2017) 258-265.  
280 <http://dx.doi.org/10.1016/j.supflu.2016.05.024>.

281 [6] S. Varona, A. Martín, M.J. Cocero, T. Gamse, Supercritical carbon dioxide fractionation  
282 of Lavandin essential oil: Experiments and modeling, J. Supercrit. Fluids 45 (2008) 181-188.  
283 <https://doi.org/10.1016/j.supflu.2007.07.010>.

284 [7] A. Martín and M.J. Cocero, Mathematical modeling of the fractionation of liquids with  
285 supercritical CO<sub>2</sub> in a countercurrent packed column, J. Supercrit. Fluids 39 (2007) 304-314.  
286 <https://doi.org/10.1016/j.supflu.2006.03.004>.

287 [8] A. Kremser, Theoretical analysis of absorption columns, Nat. Petroleum News, 22 (1930),  
288 43-49.

- 289 [9] W.C. Edmister, Absorption and stripping-factor functions for distillation calculation by  
290 manual- and digital-computer methods, *AIChE J.* 3 (1957), 165-171.  
291 <https://doi.org/10.1002/aic.690030207>.
- 292 [10] E. Henley and J. Seader, *Approximate Methods for Multicomponent, Multistage*  
293 *Separations*, in: *Equilibrium-stage separation operations in chemical engineering*. Wiley,  
294 1981, pp. 427-500.
- 295 [11] G. Brunner, Counter-current separations, *J. Supercrit. Fluids* 47 (2009) 574-582.  
296 <https://doi.org/10.1016/j.supflu.2008.09.022>.
- 297 [12] A. Bejarano, P.C. Simões, J.M. del Valle, Fractionation technologies for liquid mixtures  
298 using dense carbon dioxide, *J. Supercrit. Fluids* 107 (2016) 321-348.  
299 <http://dx.doi.org/10.1016/j.supflu.2015.09.021>.
- 300 [13] C.A. Pieck, C. Crampon, F. Charton, E. Badens, Multi-scale experimental study and  
301 modeling of the supercritical fractionation process, *J. Supercrit. Fluids* 105 (2015), 158-169.  
302 <http://dx.doi.org/10.1016/j.supflu.2015.01.021>.
- 303 [14] C. Dufour, C. Crampon, C. Delbecque, P.-P. Garry, E. Badens, Purification of sclareol by  
304 supercritical CO<sub>2</sub> fractionation process, *J. Supercrit. Fluids* 122 (2017) 35-42.  
305 <http://dx.doi.org/10.1016/j.supflu.2016.12.001>.

306

307

## Figure captions

**Fig. 1.** Sclareol skeletal formula.

**Fig. 2.** Supercritical fluid fractionation unit.

**Fig. 3.** Evolution of the mass fraction of sclareol (a) in the extract at 313 K ( $\circ$ ), 323 K ( $\Delta$ ), and 338 K ( $\square$ ) and in the raffinate at 313 K ( $\bullet$ ), 323 K ( $\blacktriangle$ ), and 338 K ( $\blacksquare$ ) versus  $\text{CO}_2$ -over-feed ratio ( $S/Z$ ) when pressure is set to 10 MPa; evolution of the yield in sclareol (b) in the raffinate versus the ratio  $R/(R+E)$  at 10 MPa and for temperatures of 313 K ( $\bullet$ ), 323 K ( $\blacktriangle$ ), and 338 K ( $\blacksquare$ ).

**Fig. 4.** Evolution of the mass fraction of sclareol (a) in the extract at 10 MPa ( $\circ$ ), 11 MPa ( $\square$ ), and 12 MPa ( $\Delta$ ) and in the raffinate at 10 MPa ( $\bullet$ ), 11 MPa ( $\blacksquare$ ), and 12 MPa ( $\blacktriangle$ ) versus  $\text{CO}_2$ -over-feed ratio ( $S/Z$ ) when temperature is set to 338 K; evolution of the yield in sclareol (b) in the raffinate versus the ratio  $R/(R+E)$  at 338 K and for pressures of 10 MPa ( $\bullet$ ), 11 MPa ( $\blacksquare$ ), and 12 MPa ( $\blacktriangle$ ).

**Fig. 5.** Evolution of the mass fraction of sclareol (a) in the extract at 10 MPa ( $\circ$ ), 11 MPa ( $\square$ ), and 12 MPa ( $\Delta$ ) and in the raffinate at 10 MPa ( $\bullet$ ), 11 MPa ( $\blacksquare$ ), and 12 MPa ( $\blacktriangle$ ) versus  $\text{CO}_2$ -over-feed ratio ( $S/Z$ ) when temperature is set to 323 K; evolution of the yield in sclareol (b) in the raffinate versus the ratio  $R/(R+E)$  at 323 K and for pressures of 10 MPa ( $\bullet$ ), 11 MPa ( $\blacksquare$ ), and 12 MPa ( $\blacktriangle$ ).

**Fig. 6.** Chromatographic profile of the feed containing about 24% of sclareol with an identification of the 12 selected compounds. Refer to Table 3 for peak identification.

**Fig. 7.** Mass balance checking for the essays performed at 10 MPa and 323 K – Calculated global fraction in the feed  $(X_i^Z)_{calc}$  versus the experimental one  $(X_i^Z)_{exp}$ . The slope of the straight line is equal to 1.0081 and the regression parameter is equal to 0.9962.

**Fig. 8.** Extraction yield versus the CO<sub>2</sub>-over-feed ratio at 323 K and 10 MPa – the slope of the straight line is equal to 0.004 and the regression coefficient R<sup>2</sup> is equal to 0.9761.

**Fig. 9.** Evolution of the raffinate and extract composition of I1 (a), I2 (b), I3 (c), I4 (d), I5 (e), I6 (f), I7 (g), I8 (h), I9 (i), I10 (j), I11 (k), and sclareol (l) versus extract yield for a fractionation performed under 10 MPa and a temperature of 323 K. Model output is represented by dashed (extract) and full (raffinate) lines. Squares represent experimental raffinate and circles represent experimental extract.

**Fig. 10.** Comparison between experimental and calculated compositions in the extract and the raffinate - Operating conditions: 323 K for pressures of 10 MPa and 11 MPa, and 338 K for a pressure of 12 MPa.



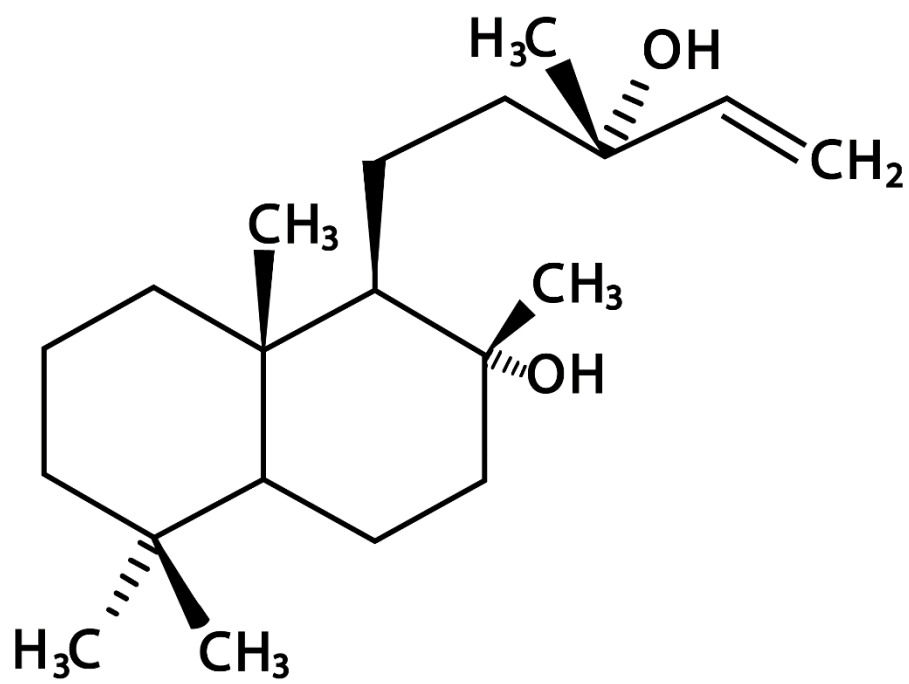


**Fig. 1.** Sclareol skeletal formula

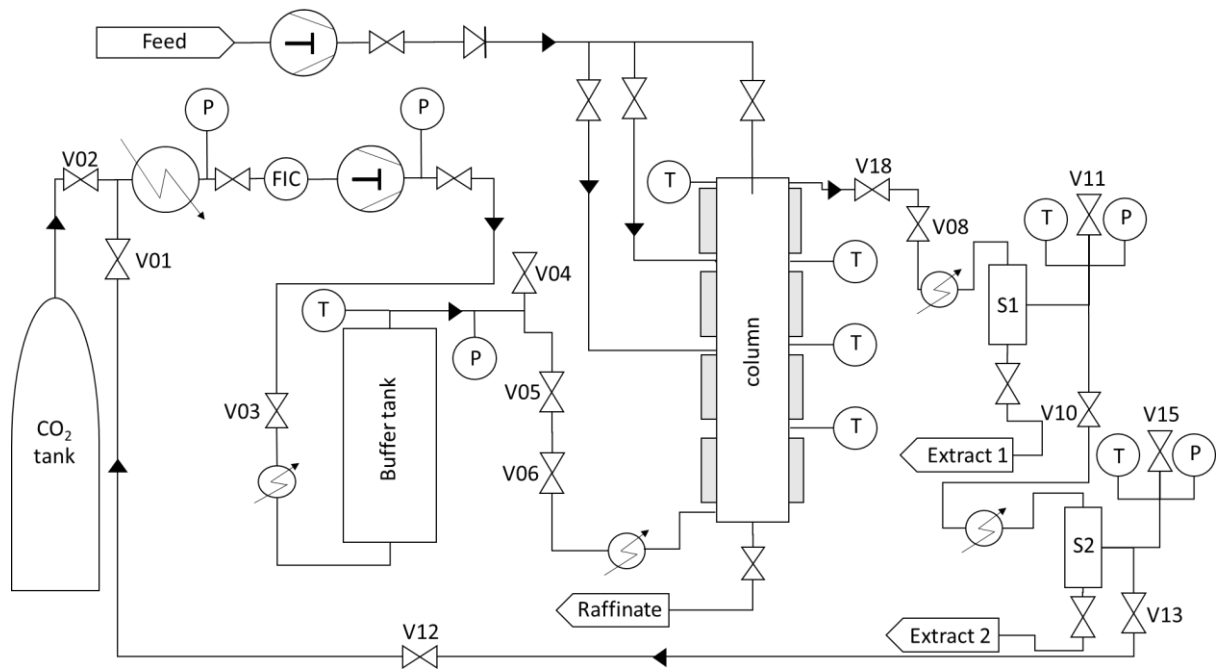


**Fig. 2.** Supercritical fluid fractionation set-up

V01 to V18 are valves; S1 and S2 are separators; T, P are temperature and pressure sensors

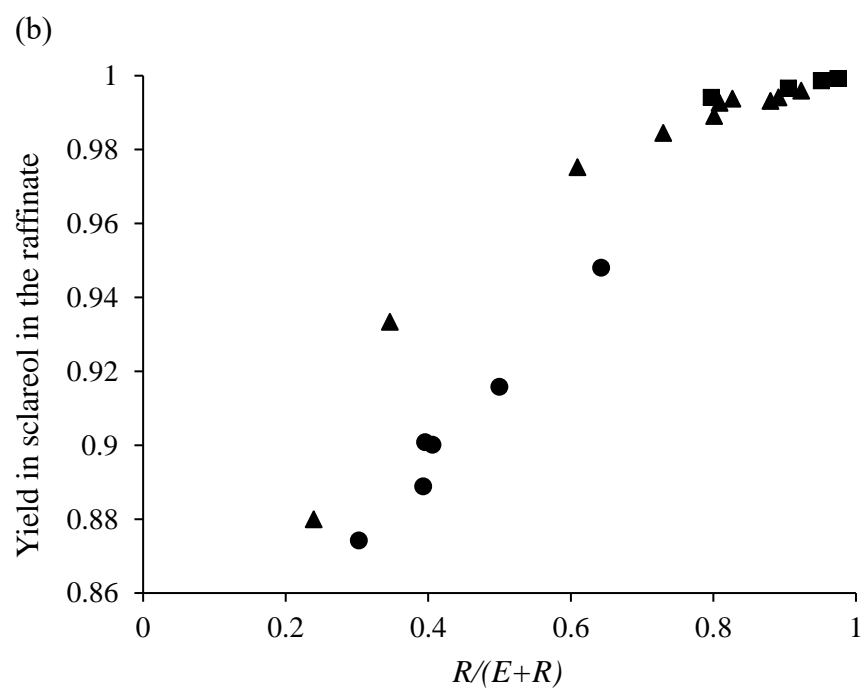
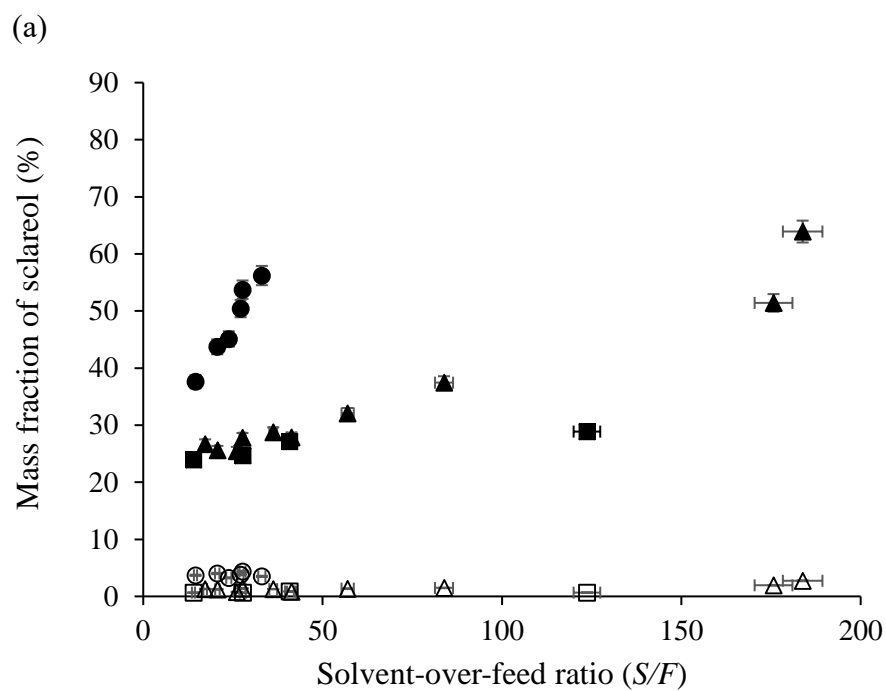


**Fig. 3.** Evolution of the mass fraction of sclareol (a) in the extract at 313 K ( $\circ$ ), 323 K ( $\Delta$ ), and 338 K ( $\square$ ) and in the raffinate at 313 K ( $\bullet$ ), 323 K ( $\blacktriangle$ ), and 338 K ( $\blacksquare$ ) versus  $\text{CO}_2$ -over-feed ratio ( $S/Z$ ) when pressure is set to 10 MPa; evolution of the yield in sclareol (b) in the raffinate versus the ratio  $R/(R+E)$  at 10 MPa and for temperatures of 313 K ( $\bullet$ ), 323 K ( $\blacktriangle$ ), and 338 K ( $\blacksquare$ ).

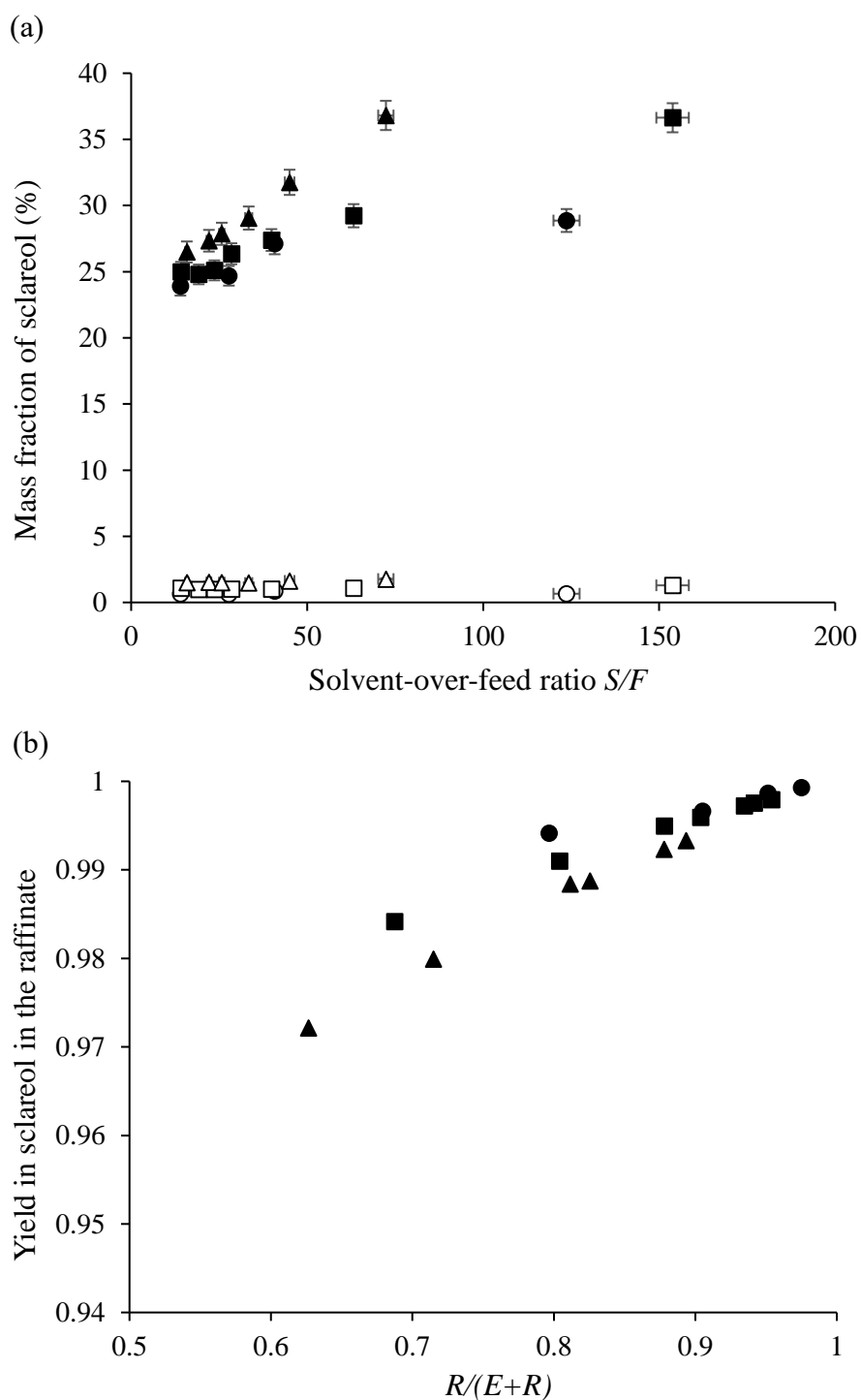


**Fig. 4.** Evolution of the mass fraction of sclareol (a) in the extract at 10 MPa (○), 11 MPa (□), and 12 MPa (△) and in the raffinate at 10 MPa (●), 11 MPa (■), and 12 MPa (▲) versus  $\text{CO}_2$ -over-feed ratio ( $S/Z$ ) when temperature is set to 338 K; evolution of the yield in sclareol (b) in the raffinate versus the ratio  $R/(R+E)$  at 338 K and for pressures of 10 MPa (●), 11 MPa (■), and 12 MPa (▲).

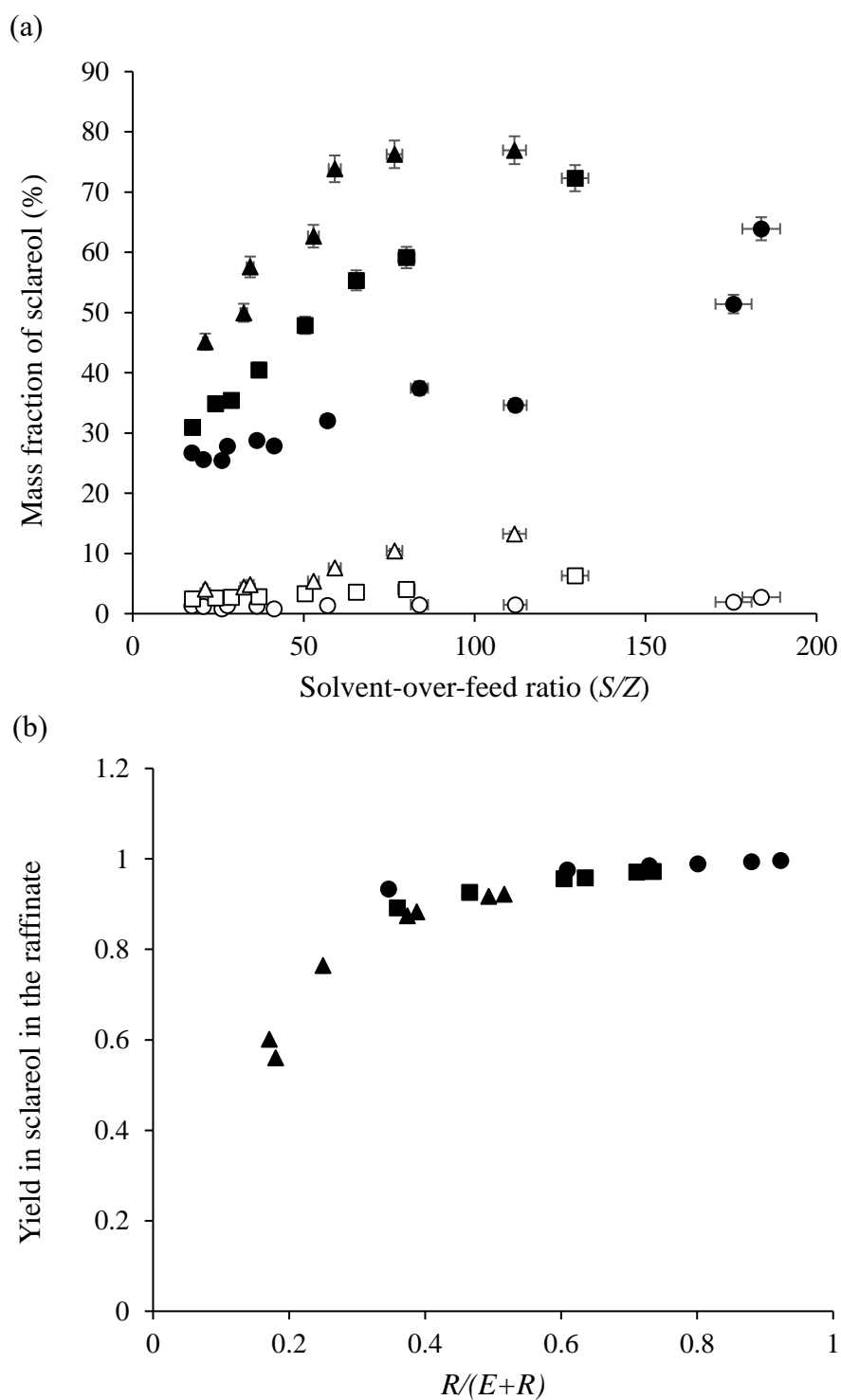


**Fig. 5.** Evolution of the mass fraction of sclareol (a) in the extract at 10 MPa ( $\circ$ ), 11 MPa ( $\square$ ), and 12 MPa ( $\Delta$ ) and in the raffinate at 10 MPa ( $\bullet$ ), 11 MPa ( $\blacksquare$ ), and 12 MPa ( $\blacktriangle$ ) versus  $\text{CO}_2$ -over-feed ratio ( $S/Z$ ) when temperature is set to 323 K; evolution of the yield in sclareol (b) in the raffinate versus the ratio  $R/(E+R)$  at 323 K and for pressures of 10 MPa ( $\bullet$ ), 11 MPa ( $\blacksquare$ ), and 12 MPa ( $\blacktriangle$ ).

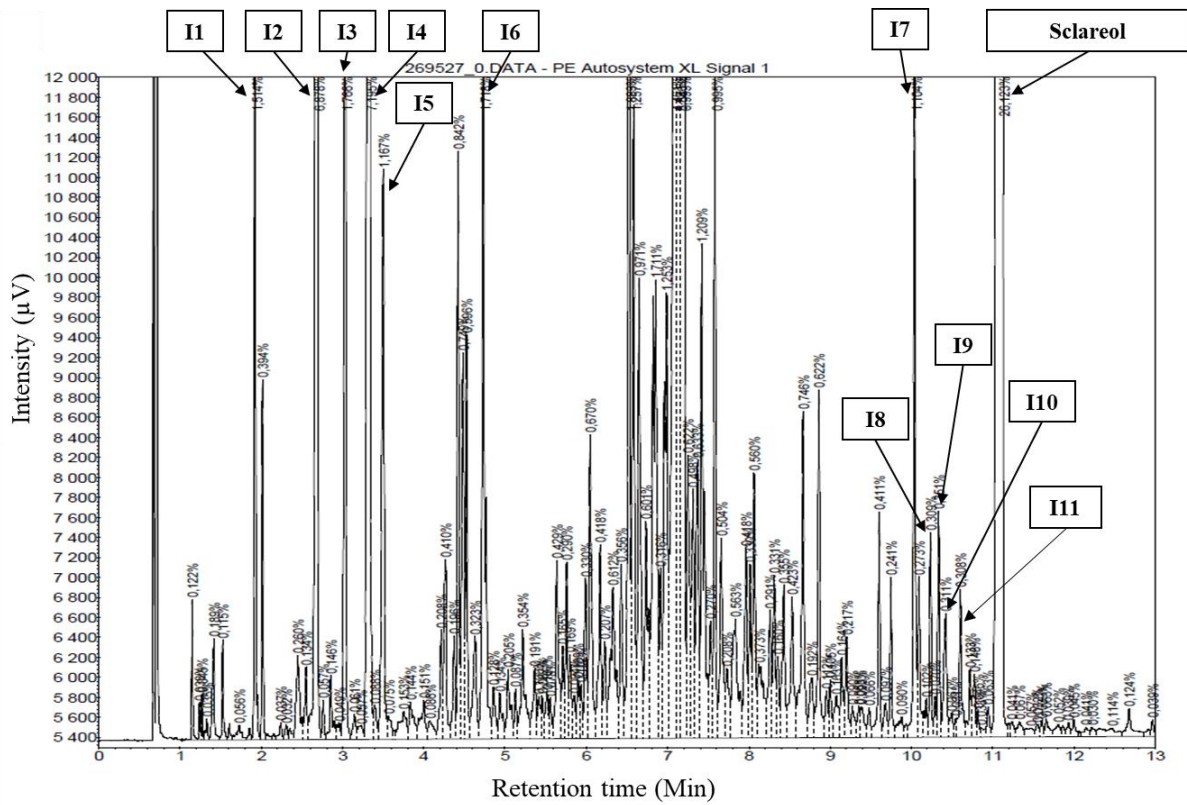


**Fig. 6.** Chromatographic profile of the feed containing about 24% of sclareol with an identification of the 12 selected compounds. Refer to Table 3 for peak identification.

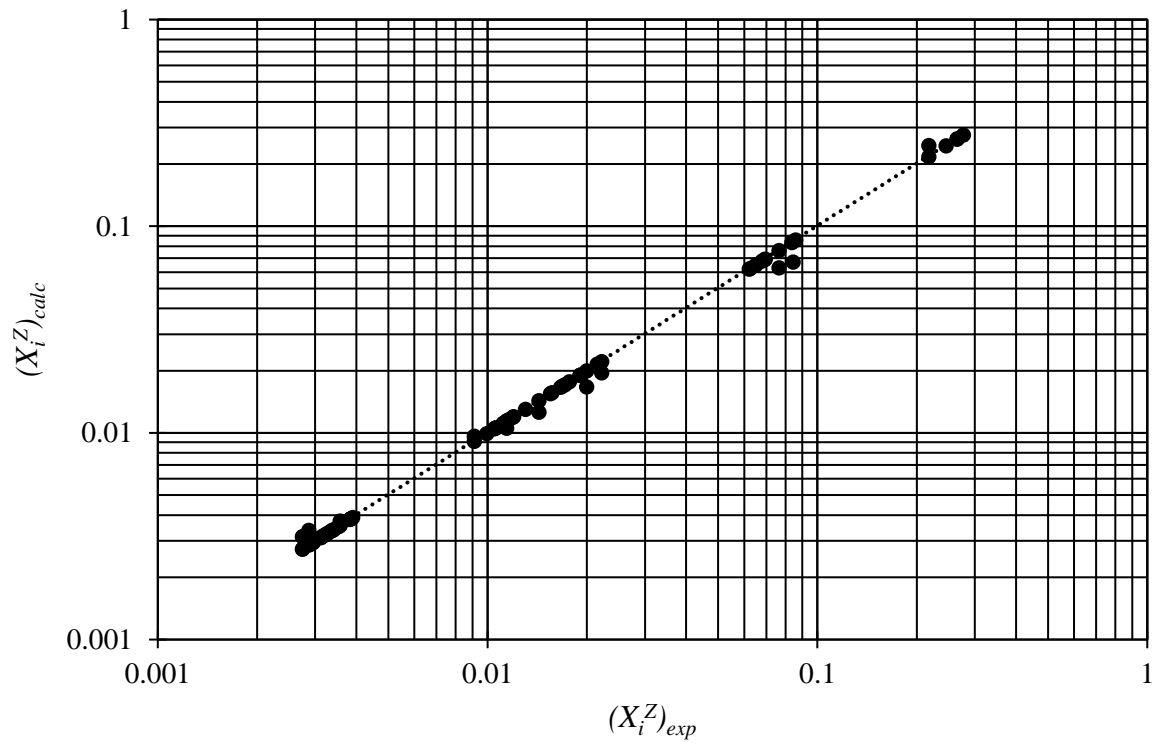


**Fig. 7.** Mass balance checking for the essays performed at 10 MPa and 323 K – Calculated global fraction in the feed  $(X_i^Z)_{calc}$  versus the experimental one  $(X_i^Z)_{exp}$ . The slope of the straight line is equal to 1.0081 and the regression parameter is equal to 0.9962.

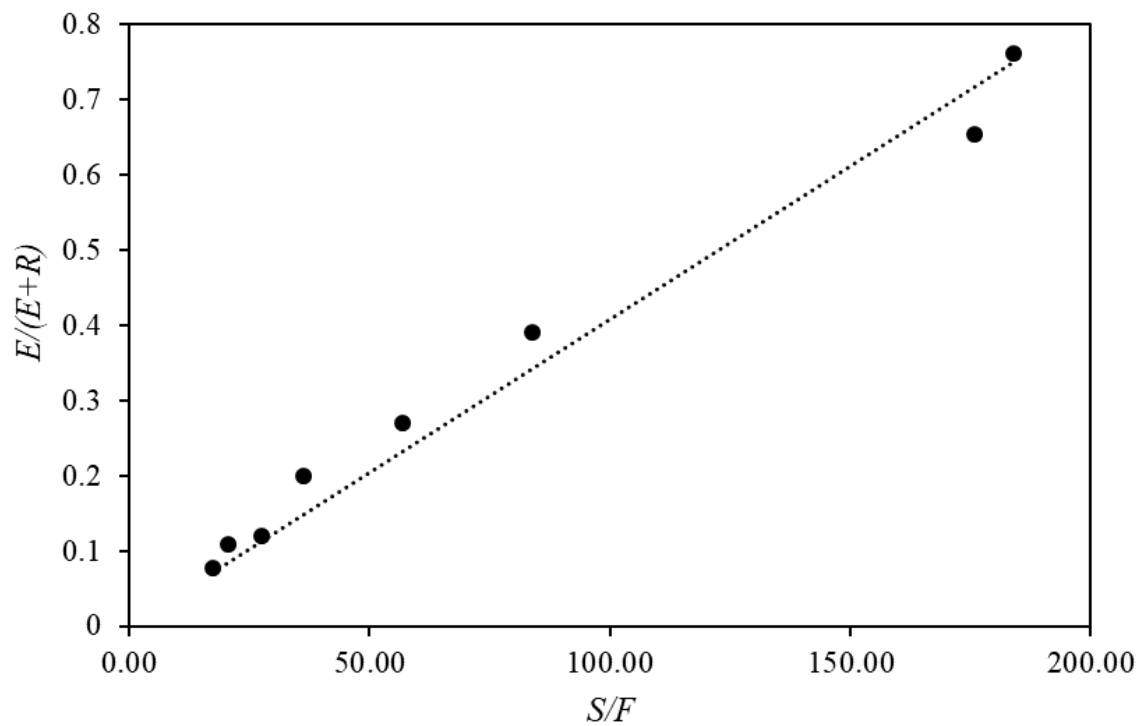


**Fig. 8.** Extraction yield versus the CO<sub>2</sub>-over-feed ratio at 323 K and 10 MPa – the slope of the straight line is equal to 0.004 and the regression coefficient  $R^2$  is equal to 0.9761



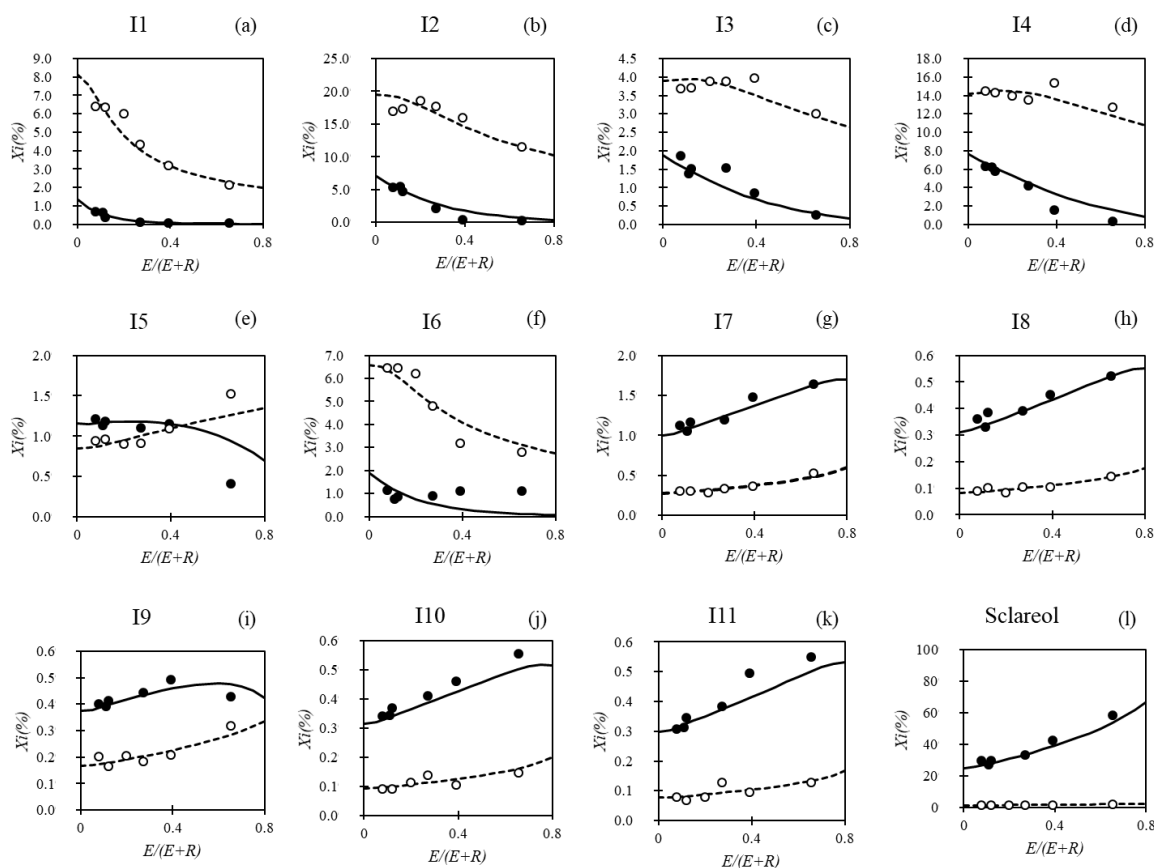


**Fig. 9.** Evolution of the raffinate and extract composition of I1 (a), I2 (b), I3 (c), I4 (d), I5 (e), I6 (f), I7 (g), I8 (h), I9 (i), I10 (j), I11 (k), and sclareol (l) versus extract yield for a fractionation performed under 10 MPa and a temperature of 323 K. Model output is represented by dashed (extract) and full (raffinate) lines. Squares represent experimental raffinate and circles represent experimental extract.

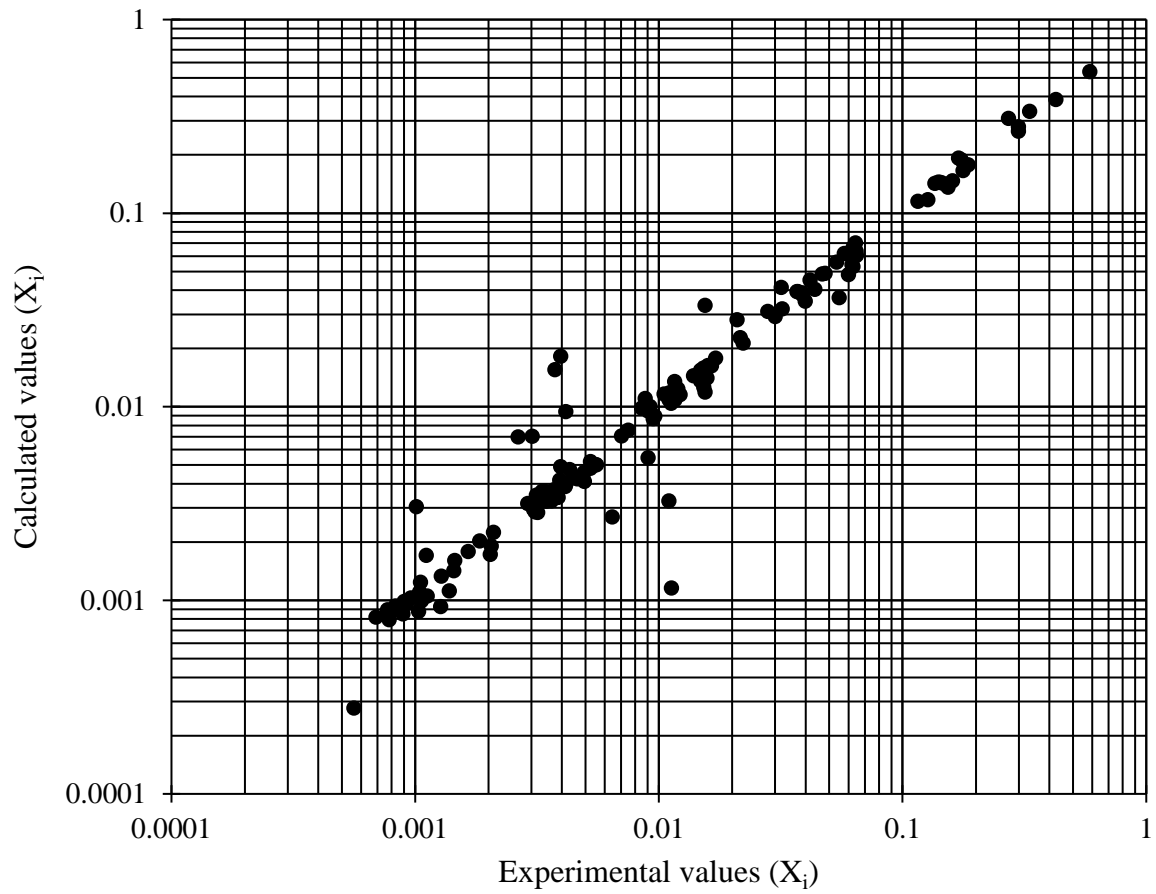


**Fig. 10.** Comparison between experimental and calculated compositions in the extract and the raffinate - Operating conditions: 323 K for pressures of 10 MPa and 11 MPa, and 338 K for a pressure of 12 MPa.

## List of tables

**Table 1.** Table 1. Experimental results obtained for operating conditions studied. \*Supercritical solvent free mass fractions; \*\* $\beta$ : partial mass balance in sclareol.

**Table 2:** Compounds selected for the modeling and their respective compositions in the feed -  
NI = Not Identified

**Table 3.** Distribution coefficients  $K_i$  and number of theoretical stages  $n$  obtained for each operating conditions

**Table 1.** Experimental results obtained for operating conditions studied. \*Supercritical solvent free mass fractions; \*\* $\beta$ : partial mass balance in sclareol

<i>P</i>	<i>T</i>	<i>S</i>	<i>Z</i>	<i>X<sub>Z</sub></i>	<i>E</i>	<i>X<sub>E</sub>*</i>	<i>R</i>	<i>X<sub>R</sub>*</i>	$\beta^{**}$	$\tau$	
(MPa)	(K)	(kg·h <sup>-1</sup> )	(kg·h <sup>-1</sup> )	(%)	(kg·h <sup>-1</sup> )	(%)	(kg·h <sup>-1</sup> )	(%)		(%)	
<b>10</b>	338	27	1.93	23.3	0.049	0.7	1.88	23.9	0.99	99.9	
		27	0.22	23.3	0.044	0.7	0.17	28.9	0.96	99.4	
		27	0.97	23.3	0.048	0.6	0.93	24.7	1	99.8	
		20	0.49	24.3	0.047	0.9	0.44	27.1	1	99.7	
		40	1.43	24.0	0.26	1.6	1.17	27.6	0.95	98.7	
		40	0.68	24.0	0.23	1.7	0.44	35.6	0.98	97.5	
	323	20	1.16	24.5	0.089	1.3	1.07	26.7	1	99.6	
		20	0.72	24.1	0.087	1.4	0.64	27.8	1	99.3	
		20	0.55	22.7	0.11	1.3	0.44	28.8	1	98.9	
		40	0.70	23.3	0.19	1.4	0.51	32.0	1	98.4	
		40	0.48	21.4	0.19	1.5	0.29	37.4	1	97.5	
		40	0.23	21.4	0.15	1.9	0.079	51.4	0.88	93.3	
	313	20	1.37	24.5	0.49	3.7	0.88	37.6	1	94.8	
		20	0.56	24.5	0.27	4.1	0.28	49.9	1	92.5	
		40	1.94	24.3	0.97	4.0	0.97	43.7	0.98	91.6	
		40	1.44	21.7	0.88	4.3	0.57	53.7	1	88.9	
		40	1.47	22.0	0.87	3.8	0.60	50.4	1	90.0	
		40	1.68	19.5	1.01	3.2	0.66	45.1	1	90.0	
		40	1.17	19.5	0.69	3.6	0.47	49.8	1	90.6	
		40	1.21	18.1	0.84	3.5	0.37	56.2	1	87.4	
	<b>11</b>	338	27	1.91	23.9	0.088	1.1	1.82	25.0	0.99	99.8
			27	1.41	23.9	0.082	1.0	1.32	24.8	0.97	99.8
			27	1.14	23.9	0.075	1.0	1.07	25.1	0.99	99.7
			27	0.95	23.9	0.091	1.0	0.86	26.4	1	99.6
			27	0.68	23.9	0.083	1.0	0.59	27.4	0.99	99.5
			27	0.43	23.8	0.083	1.1	0.34	29.2	0.98	99.1
			27	0.18	23.8	0.055	1.3	0.12	36.6	1	98.4
		323	34	1.94	24.6	0.51	2.5	1.43	30.9	0.95	97.2
34			1.41	24.6	0.41	2.6	1.00	34.9	1	97.0	
34			1.18	24.4	0.43	2.7	0.75	35.4	0.96	95.8	
34			1.41	24.6	0.41	2.6	1.00	34.9	1	97.0	
34			1.18	24.4	0.43	2.7	0.75	35.4	0.96	95.8	
34			0.92	24.4	0.36	2.8	0.56	40.5	1	95.6	
34			0.67	24.4	0.36	3.3	0.31	47.9	0.98	92.6	
<b>12</b>	338	30	1.89	24.6	0.20	1.5	1.69	26.5	0.97	99.3	
		30	1.36	24.6	0.17	1.5	1.19	27.3	0.98	99.2	
		30	1.16	23.1	0.20	1.5	0.96	27.9	1	98.9	
		30	0.90	23.1	0.17	1.5	0.73	29.1	1	98.8	
		30	0.67	23.2	0.19	1.6	0.48	31.8	1	97.9	
		30	0.41	23.2	0.15	1.7	0.26	36.8	1	97.2	
	323	40	1.89	23.7	0.91	4.1	0.97	45.2	1	92.1	
		40	1.23	23.7	0.62	4.4	0.61	49.9	1	91.7	
		40	1.16	29.8	0.71	4.8	0.45	57.6	0.88	88.3	
		40	0.76	29.8	0.47	5.4	0.28	62.7	0.89	87.4	
		40	0.68	24.1	0.51	7.6	0.17	73.9	1	76.4	
		40	0.36	24.1	0.29	13.3	0.065	76.9	1	56.0	
		40	0.52	23.5	0.43	10.5	0.089	76.3	0.93	60.1	

**Table 2:** Compounds selected for the modeling and their respective compositions in the feed -

NI = Not Identified

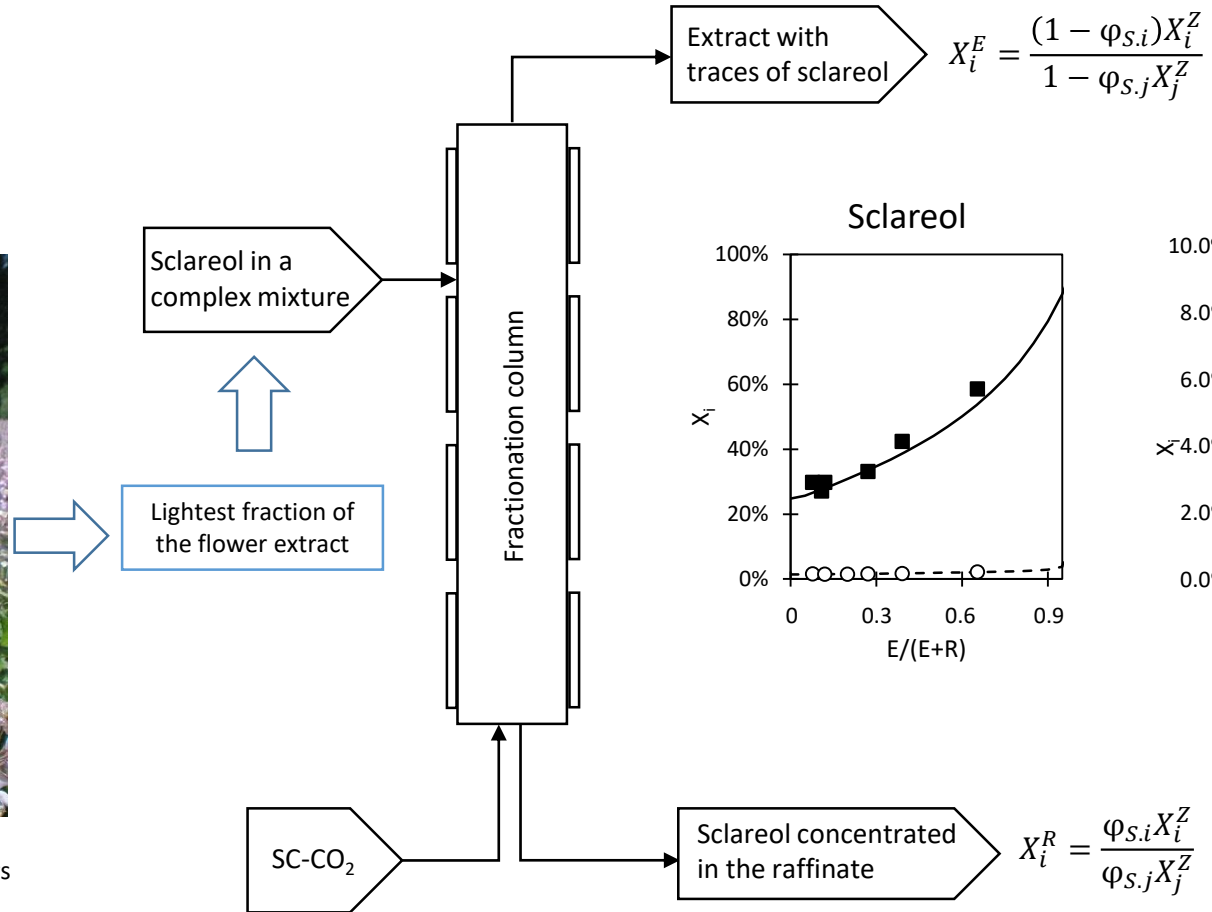
Reference code	Name of selected compound	Overall estimated mass fraction in the feed (%)
I <sub>1</sub>	Linalool	1.36
I <sub>2</sub>	Alpha terpineol	7.14
I <sub>3</sub>	Nerol	1.87
I <sub>4</sub>	Linalyl acetate + geraniol	7.64
I <sub>5</sub>	NI	1.16
I <sub>6</sub>	NI	1.89
I <sub>7</sub>	NI	0.99
I <sub>8</sub>	NI	0.31
I <sub>9</sub>	NI	0.37
I <sub>10</sub>	NI	0.31
I <sub>11</sub>	NI	0.29
Sclareol	Sclareol	24.2

**Table 3.** Distribution coefficients  $K_i$  and number of theoretical stages  $n$  obtained for each operating conditions

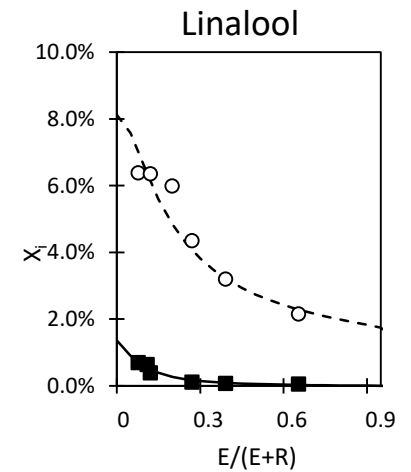
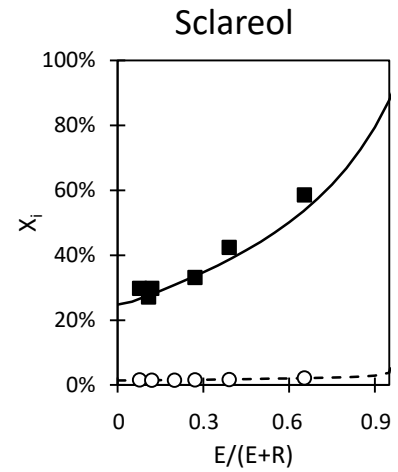
Reference code	Distribution coefficients $K_i$		
	10 MPa - 323 K $n = 2.2$	11 MPa - 323 K $n = 1.6$	12 MPa - 338 K $n = 4.1$
<b>I<sub>1</sub></b>	8.02	7.78	5.99
<b>I<sub>2</sub></b>	3.67	5.06	2.90
<b>I<sub>3</sub></b>	2.81	3.49	2.32
<b>I<sub>4</sub></b>	2.49	2.76	2.15
<b>I<sub>5</sub></b>	0.98	1.01	0.97
<b>I<sub>6</sub></b>	4.68	3.02	3.56
<b>I<sub>7</sub></b>	0.37	0.48	0.31
<b>I<sub>8</sub></b>	0.36	0.44	0.28
<b>I<sub>9</sub></b>	0.60	0.78	0.40
<b>I<sub>10</sub></b>	0.39	0.45	0.30
<b>I<sub>11</sub></b>	0.35	0.44	0.28
<b>Sclareol</b>	0.07	0.10	0.07



Clary Sage flowers



$$X_i^E = \frac{(1 - \varphi_{S,i})X_i^Z}{1 - \varphi_{S,j}X_j^Z}$$



$$X_i^R = \frac{\varphi_{S,i}X_i^Z}{\varphi_{S,j}X_j^Z}$$